NASA TECHNICAL MEMORANDUM

NASA TM X-73420

NASA TM X-73420

NOZZLE AND WING GEOMETRY EFFECTS ON OTW AERODYNAMIC CHARACTERISTICS

by U. von Glahn and D. Groesbeck
Lewis Research Center
Cleveland, Ohio 44135

TECHNICAL PAPER to be presented at
Twelfth Propulsion Conference cosponsored
by the American Institute of Aeronautics and
Astronautics and the Society of Automotive Engineers
Palo Alto, California, July 26-29, 1976

NOZZLE AND WING GEOMETRY EFFECTS ON OTW AERODYNAMIC CHARACTERISTICS

U. von Glahn* and D. Groesbeck**
National Aeronautics and Space Administration
Lewis Research Center
Cleveland, Ohio 44135

ABSTRACT

The effects of nozzle geometry and wing size on the aerodynamic performance of several 5:1 aspect ratio slot nozzles are presented for OTW configurations. Nozzle geometry variables include roof angle, sidewall cutback, and nozzle chordwise location. Wing variables include chord size, and flap deflection. Several external deflectors also were included for comparison. The data indicate that good flow turning may not necessarily provide the best aerodynamic performance. The results of the study suggest that a variable exhaust nozzle geometry offers the best solution for a viable OTW configuration.

E-8758

INTRODUCTION

In order to attach the flow from the exhaust of an engine-over-the-wing configuration to the wing and flap surfaces, two general nozzle design classes are usually considered. The first nozzle design class consists of a nozzle which is mounted flush to the wing surface (fig. 1(a)). In order to provide flow attachment to the wing, the nozzle is usually D-shaped or a slot nozzle. Furthermore, in order to enhance flow attachment, the roof of the nozzle is canted or sloped toward the wing surface and is considered to act as an internal deflector. In order to provide a greater spreading of the exhaust flow spanwise over the wing and flap surfaces, the sidewalls of the nozzle can be flared or cutback. By increasing the spread of the flow over more of the wing and flap surfaces, the flow velocity at the trailing edge is reduced and a lower noise level is obtained[1]. However, the increased spread of the exhaust flow over the surfaces also affects the aerodynamic performance of the nozzle/wing system. The second nozzle design class consists of nozzles to which external deflectors are attached to vector the exhaust flow toward the surface (fig. 1(b)). This type of nozzle/deflector configuration also tends to spread the flow spanwise over the wing and flap surfaces, thereby reducing the trailing-edge peak velocity and associated noise levels[1].

It is the purpose of this paper to examine the effects of nozzle geometry and wing size on the aerodynamic performance, including lift and thrust measurements of several 5:1 aspect ratio slot nozzles in over-the-wing configurations. Considered are the effect on the nozzle/wing aerodynamic characteristics of changes in nozzle roof (kickdown) angle, chord length, flap deflection, and location of the nozzle exhaust plane relative to the flap trailing edge. A 5:1 slot nozzle with an equivalent diameter of 5.1 centimeter was used in the work. Nozzle roof angles were varied from 10° to 40° relative to the wing chordline. The nozzle sides in the exhaust plane were either normal to the shielding surface or cutback to be normal to the nozzle roof. In addition, several external deflectors[1] were also included for comparison purposes in the study. Projected surface shielding lengths (parallel to the chordline) were varied from about 18 to 58 centimeters, and flap deflection angles of 20° and 60° were used. The nozzle exhaust plane was located at the nominal 21% chord station of the wing and at the beginning of the flap location (approximately 46% of the wing chord). As discussed in reference 1, the relative sizes of the nozzle to the various shielding surface lengths simulate the effect of engine configurations on a twin engine aircraft (baseline wing), a single engine pod of a four-engine aircraft (3/2-baseline wing), and a siamese pod in which two engines exhaust from a single nozzle (2/3-baseline wing).

Aerodynamic data are presented for both nozzles only and the various nozzle/wing configurations. The data were obtained with nozzle velocities of 195 and 253 m/sec.

APPARATUS AND PROCEDURE

Facility

Aerodynamic data consisting of lift and thrust components were obtained using the test stand[2] shown in figure 2. In this test stand pressurized air at about 289 K was supplied to 15.25-centimeter diameter plenum by twin diametrically opposed supply lines. Flexible couplings in each of the twin supply lines isolate the supply system from a force measuring system. The plenum is free to move axially and laterally through an overhead cable suspension system. The test nozzles, with and without wings, were attached to a flange at the downstream end of the plenum. A load cell at the upstream end of the plenum is used to measure thrust. A second load cell is mounted near the nozzle to measure horizontal side loads. The wing-flap section was mounted in a vertical plane so that lift forces were measured by the side-mounted load cell[2]. Thrust and lift forces were obtained at nominal nozzle pressure ratios of 1.28 and 1.53 which yielded nominal jet velocities of 195 and 253 m/sec, respectively.

Airflow through the overhead supply line was measured with a calibrated orifice. The nozzle inlet total pressure was measured with a single probe near the plenum exit flange. Pressure data were recorded from suitable multitube manometers.

Local jet Mach number (velocity) measurements were obtained on the same facility at several locations downstream of the nozzle exhaust plane for the various nozzle-only configurations. Similar data were obtained at the trailing edge of the shielding surfaces. Measurements were made with a traversing pilot tube (fig. 3) with an entrance cone angle of 60° to help minimize flow angularity effects resulting from the jet flow over the curved surfaces. A vane on the traversing equipment was used to establish the jet flow angle for each traverse. When the flow angle, as determined by means of the vane, exceeded the angularity capability of the pitot tube, the tube angle to the local flow

*Member AIAA; Chief, Jet Acoustics Branch
**Aerospace Research Engineer

NOZZLE AND WING GEOMETRY EFFECTS ON OTW AERODYNAMIC CHARACTERISTICS

U. von Glahn* and D. Groesbeck**
National Aeronautics and Space Administration
Lewis Research Center
Cleveland, Ohio 44135

ABSTRACT

The effects of nozzle geometry and wing size on the aerodynamic performance of several 5:1 aspect ratio slot nozzles are presented for OTW configurations. Nozzle geometry variables include roof angle, sidewall cutback, and nozzle chordwise location. Wing variables include chord size, and flap deflection. Several external deflectors also were included for comparison. The data indicate that good flow turning may not necessarily provide the best aerodynamic performance. The results of the study suggest that a variable exhaust nozzle geometry offers the best solution for a viable OTW configuration.

E-8758

INTRODUCTION

In order to attach the flow from the exhaust of an engine-over-the-wing configuration to the wing and flap surfaces, two general nozzle design classes are usually considered. The first nozzle design class consists of a nozzle which is mounted flush to the wing surface (fig. 1(a)). In order to provide flow attachment to the wing, the nozzle is usually D-shaped or a slot nozzle. Furthermore, in order to enhance flow attachment, the roof of the nozzle is canted or sloped toward the wing surface and is considered to act as an internal deflector. In order to provide a greater spreading of the exhaust flow spanwise over the wing and flap surfaces, the sidewalls of the nozzle can be flared or cutback. By increasing the spread of the flow over more of the wing and flap surfaces, the flow velocity at the trailing edge is reduced and a lower noise level is obtained[1]. However, the increased spread of the exhaust flow over the surfaces also affects the aerodynamic performance of the nozzle/wing system. The second nozzle design class consists of nozzles to which external deflectors are attached to vector the exhaust flow toward the surface (fig. 1(b)). This type of nozzle/deflector configuration also tends to spread the flow spanwise over the wing and flap surfaces, thereby reducing the trailing-edge peak velocity and associated noise levels[1].

It is the purpose of this paper to examine the effects of nozzle geometry and wing size on the aerodynamic performance, including lift and thrust measurements of several 5:1 aspect ratio slot nozzles in over-the-wing configurations. Considered are the effect on the nozzle/wing aerodynamic characteristics of changes in nozzle roof (kickdown) angle, chord length, flap deflection, and location of the nozzle exhaust plane relative to the flap trailing edge. A 5:1 slot nozzle with an equivalent diameter of 5.1 centimeter was used in the work. Nozzle roof angles were varied from 10° to 40° relative to the wing chordline. The nozzle sides in the exhaust plane were either normal to the shielding surface or cutback to be normal to the nozzle roof. In addition, several external deflectors[1] were also included for comparison purposes in the study. Projected surface shielding lengths (parallel to the chordline) were varied from about 18 to 58 centimeters, and flap deflection angles of 20° and 60° were used. The nozzle exhaust plane was located at the nominal 21% chord station of the wing and at the beginning of the flap location (approximately 46% of the wing chord). As discussed in reference 1, the relative sizes of the nozzle to the various shielding surface lengths simulate the effect of engine configurations on a twin engine aircraft (baseline wing), a single engine pod of a four-engine aircraft (3/2-baseline wing), and a siamese pod in which two engines exhaust from a single nozzle (2/3-baseline wing).

Aerodynamic data are presented for both nozzles only and the various nozzle/wing configurations. The data were obtained with nozzle velocities of 195 and 253 m/sec.

APPARATUS AND PROCEDURE

Facility

Aerodynamic data consisting of lift and thrust components were obtained using the test stand[2] shown in figure 2. In this test stand pressurized air at about 289 K was supplied to 15.25-centimeter diameter plenum by twin diametrically opposed supply lines. Flexible couplings in each of the twin supply lines isolate the supply system from a force measuring system. The plenum is free to move axially and laterally through an overhead cable suspension system. The test nozzles, with and without wings, were attached to a flange at the downstream end of the plenum. A load cell at the upstream end of the plenum is used to measure thrust. A second load cell is mounted near the nozzle to measure horizontal side loads. The wing-flap section was mounted in a vertical plane so that lift forces were measured by the side-mounted load cell[2]. Thrust and lift forces were obtained at nominal nozzle pressure ratios of 1.28 and 1.53 which yielded nominal jet velocities of 195 and 253 m/sec, respectively.

Airflow through the overhead supply line was measured with a calibrated orifice. The nozzle inlet total pressure was measured with a single probe near the plenum exit flange. Pressure data were recorded from suitable multitube manometers.

Local jet Mach number (velocity) measurements were obtained on the same facility at several locations downstream of the nozzle exhaust plane for the various nozzle-only configurations. Similar data were obtained at the trailing edge of the shielding surfaces. Measurements were made with a traversing pilot tube (fig. 3) with an entrance cone angle of 60° to help minimize flow angularity effects resulting from the jet flow over the curved surfaces. A vane on the traversing equipment was used to establish the jet flow angle for each traverse. When the flow angle, as determined by means of the vane, exceeded the angularity capability of the pitot tube, the tube angle to the local flow

*Member AIAA; Chief, Jet Acoustics Branch
**Aerospace Research Engineer

was adjusted to provide suitable data. The pressures measured were transmitted to an x-y-y' plotter which yielded direct traces on graph paper of the total pressure distribution across the jet. From these traces, velocity contour maps and trailing edge velocity profiles at the nozzle centerline were made. The velocity data were obtained with a nominal jet exhaust velocity of 253 m/sec.

Models

Wings. - The wings (shielding surfaces) are shown schematically in figure 4 together with pertinent dimensions. The surfaces consisted of metal plates secured to wooden ribs (fig. 3). The surfaces approximated the upper surface contours of the airfoil with 20° and 60° deflected flaps used in references 3 and 4.

All wings had a span of 61 centimeters. As indicated in figure 4, the nozzles were located at two axial locations on the surfaces corresponding to nominal airfoil chordwise stations of 21- and 46-percent with flaps retracted.

The wings will be referred to by the flap deflection angle, 20° or 60°, and their relative size given by 2/3-baseline, baseline and 3/2-baseline. The equivalent flaps-retracted chord sizes for these wings are 22, 33, and 49.5 centimeters, respectively.

Nozzles. - The test nozzles consisted of the 5:1 slot nozzles shown in figure 5 (see also ref. 1). The nozzles all had equivalent diameters of 5.1 centimeters. A single straight-sided nozzle was used for the tests without nozzle sidewall cutback (fig. 5(a)). The roof angle, β, for this nozzle was changed by providing inserts that altered the angle from 10° to 40° in 10° increments. Separate nozzles were provided for the cases with sidewall cutback (fig. 5(b) to 5(e)). The sidewall cutback angle, γ, was the same as the roof angle for each respective nozzle. The sidewalls of all these nozzles were parallel.

In addition to the preceding nozzles, two larger nozzles similar to that shown in figure 5(e) were also tested. These nozzles had exhaust areas 16.3 and 30 percent larger than that in figure 5(e).

A simple 5:1 slot nozzle[1] was used with various external deflectors to turn the flow (fig. 4(f)). Each of the sides of the nozzle converged at 5° and the nominal nozzle dimensions at the exhaust plane was 2.0 centimeters by 10.2 centimeters. The 40° full-lip deflector was similar to that used in reference 2.

The nozzles are referred to by their roof and cutback angles; for example, the nozzle with a 20° roof angle and 20° sidewall cutback angle is designated by "20/20" while the nozzle with a roof angle of 20° and no sidewall cutback is designated by "20/0".

RESULTS

The overall results of this study showed that all the measured aerodynamic characteristics were a function of weight flow reductions caused by the nozzle-only geometry as well as the flow interaction of nozzle flows with the wings. Consequently, because of this phenomenum, the present results will be discussed in the following order of interest and/or importance: weight flow considerations, lift and thrust measurements, trailing edge centerline velocity profiles, and flow velocity decay. The profile and decay data were needed for analyses of the acoustic characteristics for these nozzle/wing configurations reported in reference 5.

Weight Flow Considerations

The present study showed that all configurations except the baseline 5:1 slot nozzle suffered weight flow reductions when compared to calculated ideal weight flows. In the following sections, these measured weight flows are discussed and simple empirical equations are given from which the measured weight flow can be corrected to ideal flow values for the various nozzle only and nozzle/wing configurations tested.

Nozzle only. - Representative weight flow data for nozzles only, with and without sidewall cutback are shown in figure 6. The weight flow ratio W/W_i is shown plotted as a function of roof angle, β. The data shown were obtained with a nominal jet Mach number of 0.8. A comparison of the data obtained with the two types of nozzles shows that greater weight flow reductions with increasing roof angle occurred with nozzles having sidewall cutback than those without cutback. Also shown in figure 6 are calculated weight flow curves based on an empirical equation (developed from the present data) given by:

$$\frac{W}{W_i} = 1 - 0.33\,(1 - \cos\beta\sqrt{\cos\gamma}) \qquad (1)$$

The decreases in weight flow with increasing nozzle roof angle and with sidewall cutback are attributed to reductions in the vena contracta downstream of the nozzle exhaust plane caused by these geometry variations. The change in the vena contracta is reflected by a reduction in the measured weight flow. In addition, flow pressure losses within the nozzle caused by the curvature of the nozzle (roof angle) also contribute to the weight flow reductions for a given pressure ratio across the nozzle.

Nozzle/wing configuration. - The effect on weight flow caused by the various nozzle/wing configurations (excluding those using external flow deflectors) is shown in figure 7. The measured data are shown in terms of W/W_i as a function of surface length ratio, L/h, for a nominal jet Mach number of 0.8. It is apparent, from figure 7, that W/W_i for the nozzle wing configurations also decreases with increasing roof and sidewall angles. However, there are no apparent effects on weight flow caused by a change in wing size of flap deflection angle. With an increase in nozzle size, as in the case of the larger versions of the nozzle shown in figure 5(e), the weight flow obviously increased. With a 30-percent increase in nozzle size and the 3/2-baseline wing, the measured flow was equal to the ideal flow calculated for the smaller nozzle. The weight flow losses thus appear to be a local nozzle-surface interaction phenomena. The flow losses are believed to be again caused by changes in the vena contracta by the interaction of the jet exhaust flow with the local wing surface.

This nozzle-wing flow interaction results in larger weight flow reductions than those for the nozzles only, especially those with large roof angles and sidewall cutback.

Empirical relationships for predicting the W/W_i values were derived in terms of the nozzle roof and sidewall cutback angles. For the nozzles without sidewall cutback the following relationship was obtained:

$$W/W_i = 1 - 0.33\ (1 - \cos^{3/2}\ \beta) \qquad (2)$$

For the nozzles with sidewall cutback the correlating equation can be expressed by

$$W/W_i = \sqrt{\cos\ \gamma}\ \left(1 - 0.33\ (1 - \cos\ \beta\sqrt{\cos\ \gamma})\right) \qquad (3)$$

The initial $\sqrt{\cos\ \gamma}$-term in equation (3) accounts for a reduction in effective nozzle flow area (height referenced to the wing surface) for the present nozzles.

Calculated W/W_i values using the preceding equations are also shown in figure 7 for comparison with the measured data.

It should be noted that equations (2) and (3) are not applicable for very small L/h ratios. For very small L/h ratios ($<<15$) the weight flow should approach that of the nozzle only because the vena contracta should not be greatly influenced by the presence of a very short deflecting surface. The present study precludes the prediction of weight flow losses for very short L/h values. These latter are of no interest to actual OTW applications.

It should be noted that the foregoing empirical weight flow relationships apply only to the nozzle/wing configurations tested. Also, in the present study, for all the nozzles with sidewall cutback, the roof and sidewall cutback angles were the same; i.e. a 30° roof angle corresponded to a 30° sidewall cutback angle. The effect of dissimilar angles was not evaluated in the present program.

External deflectors. - The weight flow ratio, W/W_i, for the nozzle only with external deflectors (no wing) ranged from 0.989 for the full-size-lip deflectors to 0.998 for the half-size-lip deflector ($\beta = 40°$). Thus, the external deflectors used had no significant effect on the nozzle-only weight flow.

In the presence of a wing, the use of external deflectors showed somewhat higher W/W_i values (nearly 3 percentage points) than those obtained with nozzles and without sidewall cutback and having the same roof angle and lip angles. A comparison of the weight flows for these two nozzle types with comparable wings is shown in figure 8 over a range of L/h values. The curves representing the roof-angle nozzles were calculated using equation (2) with γ equal to 0° since the baseline 5:1 slot nozzle has an effective sidewall cutback angle of 0°. With the half-size-lip deflector, the weight flow ratios were substantially similar to those for the full-lip deflector with a 30° lip angle. The limited data for the external deflector configurations preclude the developing of an empirical W/W_i correlation equation.

The preceding data indicate that location of the external deflector lips still affects the weight flow and that the deflector lip should perhaps be located further downstream of the nozzle exhaust plane. Also, removal of the horizontal portion of the deflector perhaps could provide the necessary flow field relief to yield W/W_i values near 1.0 for the nozzle/wing configurations.

Lift and Thrust Characteristics

In order to provide meaningful comparisons of the aerodynamic data, all configurations are compared on the basis of equal weight flow. This, of course, does not imply equal lift and thrust.

In order to achieve equal weight flow, the nozzle area must be increased which would constitute a larger external wetted surface area resulting in a cruise-drag penalty. The latter consideration is beyond the scope of this study. The measured values of the static lift and thrust are normalized by compensating for the weight flow reductions caused by the nozzle configurations and the presence of the wing (see appendix A). The adjusted measured static lift and thrust are then ratioed to the ideal nozzle-alone thrust. These procedures led to the following expressions for the normalized lift and thrust: $L_T(W_i/W)/T_i$ and $T(W_i/W)/T_i$, respectively. The normalized data in this form are shown in figure 9. The flow turning angle shown is that made by the flow with respect to the nozzle axis. The magnitude of the vector sum of the lift and thrust, given by the magnitude of the radius, represents a flow turning efficiency.

With the 2/3-baseline wing (fig. 9) and a 20° flap deflection, the nozzle with roof angles of 20° and 30° had better aerodynamic performance (maximum considerations of lift, thrust, and turning angle) than those with roof angles of 10° and 40°. The former ($\beta = 10°$) showed low lift values while the latter ($\beta = 40°$) generally showed a somewhat lower lift than the 20° and 30° roof angles and a significant reduction in thrust. Locating the nozzle at 0.21 chord caused a reduction in turning efficiency compared to that at 0.46 chord and hence lower values of lift. In general, turning efficiencies of up to 0.93 were achieved with flow turning angles up to 28°. The maximum turning efficiency achieved with a 60° flap angle was about 0.91 with a flap turning angle of 48° to 62°.

Similar overall data trends to the preceding were also evident with the baseline and 3/2-baseline wings. With the 3/2-baseline wing, the maximum turning efficiency obtained with a 20° flap deflection was 0.90. The maximum lift was achieved with the higher nozzle roof angles of 30° and 40°, at a small reduction in turning efficiency (2-4 percent).

For the nozzles with-external-deflectors (fig. 9(b)), lift values were generally of the same order as those obtained with the other nozzle/wing configurations; however, the thrust component values were somewhat less. The largest turning angles, 31° and 64°, were obtained with the external deflectors.

The vectored thrust, T_V, (where $T_V = \sqrt{L_T^2 + T^2}$) is shown in figure 10 as a function of wing size for all the configurations tested. In general, the vectored thrust decreases with increasing wing size

(surface length). It is also apparent that the vectored thrust is a weak function of the nozzle roof angle with increasing roof angle, the vectored thrust is reduced. This reduction is more pronounced for nozzles with sidewall cutback than those without sidewall cutback. Except for the nozzles with external deflectors, the decrease in T_V with surface length is essentially independent of flap angle. The limited data with the external deflector nozzle configurations show a more rapid decrease in T_V with surface length than the other nozzle/wing configurations.

From the data shown in figures 9 and 10, a nozzle configuration for a given wing size can be selected to yield the necessary lift and thrust components for a given application. It is from these data it appears that an optimized nozzle/wing configuration may require variable nozzle geometry in order to achieve optimum aerodynamic performance.

Trailing-Edge Velocity Profiles

From the Mach number contour plots[1] taken at the flap trailing edge (see appendix B), the velocity profiles (in terms of local Mach number) was obtained at the nozzle centerline and in a direction perpendicular to the wing surface. The resulting velocity profiles were normalized by the use of δ/δ_e and M/M_p parameters as shown in figure 11. In figure 11(a) it is apparent that the shape of centerline velocity profile at a 20° flap angle is substantially independent of the nozzle roof and sidewall cutback angles. In figure 11(b), for a 60° flap angle, it is seen that the free shear layer velocity profile ($\delta/\delta_e > .4$) is independent of the nozzle geometry, but the boundary layer is influenced by nozzle geometry. The effect of wing size on the centerline velocity profile is shown in figure 11(c) and indicates substantially no effects. Similar results were obtained with a 60° flap angle. The data for the nozzles with external deflectors (figs. 11(d) and (e)) show velocity profiles similar to those not using such deflectors but having large roof and sidewall cutback angles. (The figures include the data for the 40/40 nozzle configuration for comparison.) For a 60° flap angle, (fig. 11(e)) the data with the external deflectors shows higher boundary layer velocities than those for the 40/40 nozzle, indicating better flow attachment.

An overall comparison of the profiles for flap deflections of 20° and 60° is shown in figure 11(f). It is shown that, while the profile shapes are somewhat similar, the slope of the velocity profile curve at the free shear layer is steeper for the 20° flap angle than that for the 60° flap angle. The greatest differences are seen to occur in the boundary layer. In this region the data for the configuration with nozzles having large roof and sidewall cutback angles (i.e. 40/40) have higher local boundary layer velocities than those having small roof angles and no sidewall cutback. The latter data tend to be associated with partial flow separation off the flap surface.

Correlation of δ_e. - The shear layer characteristic height, δ_e, is correlated herein by correcting the measured values for the weight flow reductions associated with the nozzle/wing configurations. This results in a normalized value of δ_e defined by δ^* as follows:

$$\delta^* = \delta_e + h \cos\gamma \sqrt{\frac{W_i}{W} - 1} \qquad (4)$$

The variation of δ^* with surface distance, L, is shown in figure 12 for representative nozzle/wing configurations. Note that both δ^* and L in figure 12 are nondimensionalized by the use of a normalized or effective nozzle height h^* that includes consideration of weight flow changes due to the configuration geometry. The h^*-term is given by:

$$h^* = h \cos\gamma \sqrt{\frac{W_i}{W}} \qquad (5)$$

As shown in figure 12, δ^* decreases with an increase in roof and sidewall cutback angles while increasing with an increase in flap detection angle. The correlation of δ^* with configuration geometry is shown in figure 13. The parameter Z includes the effects of roof angle, β, sidewall cutback angle, γ, and flap angle, α. The Z-parameter is given by:

$$Z = \frac{(1 + \sin^4\beta)(1 + \sin^3\gamma)}{(1 + \sin\alpha)^2} \qquad (6)$$

Good correlation is achieved for most of the data shown. Deviations at both ends of the data range are attributed, in part, to partial flow separation from the surfaces near the trailing edge.

Jet Velocity Decay

Nozzle only. - Representative data of the peak-axial jet velocity decay, taken in the nozzle centerline plane from velocity contour maps similar to those given in reference 1, are shown in figure 14. The data are shown in terms of the ratio M_p/M_j as a function of a velocity decay correlation parameter obtained from reference 6. The shape of the common curves drawn through the data points is that given in reference 6 for a 5:1 aspect ratio slot nozzle. The baseline 5:1 slot nozzle (circle symbols) has a coefficient of 1.0. It is apparent that even a small nozzle roof angle (10°) causes a significant decrease in the peak velocity at a given axial station compared with the baseline nozzle. With a small roof angle (10°) the effect of nozzle sidewall cutback is not apparent; however with a nozzle roof angle of 40°, sidewall cutback is seen to cause a more rapid decrease in peak velocity with axial distance than that for a nozzle without sidewall cutback. With increasing roof angle the peak velocity decreases at all axial stations.

Nozzle with wing. - The peak jet velocity decay at the trailing edge of representative wing/flap surfaces is shown in figure 15. The data were obtained in the nozzle centerline plane. The data are shown in terms of the ratio M_p/M_j as a function of $L/D_e\sqrt{1 + M_j}$ where the surface length, L, has replaced the axial distance, X, used previously in figure 14. The curves are similar in shape and are faired through the data, not curves taken from reference 6 as was the case for the nozzle only data in figure 14.

For a 20° flap angle, the peak velocity ratio M_p/M_j at a given surface station, L, is seen to

decrease with increasing roof angles (fig. 15(a)). As was the case for the nozzles-only, the jet velocity at a given value of L decreases more for a nozzle having a significant sidewall cutback (40°) compared with a similar nozzle without sidewall cutback. Shown also in figure 15 are the peak jet velocity decay data for the 5:1 baseline slot nozzle with a 40° full-lip external deflector. This configuration has a peak jet velocity decay rate about 2/3 more than the nozzle-wing configurations without an external deflector.

Although the data are more limited for the 60° flap angle, the data yield generally similar trends (fig. 15(b)).

A comparison of the jet velocity decay characteristics for nozzle/wing configurations with that for the 40/40 nozzle only is shown in figure 16. (In the abscissa, the L-term for the nozzle-only case is the axial distance, X.) It is apparent that the peak jet velocity decays less when the jet flow is attached to a surface than when the jet is free as for the nozzle only. The least jet velocity decay is noted for the 20° flap configuration. Similar trends were obtained with the other nozzle-wing configurations tested.

The data for the 40° full-lip external-deflector nozzle configuration with a 20° flap angle falls on or below the nozzle-only data in figure 16. With a 60° flap angle, the data with an external deflector fell somewhat below that for the 20° flap data for the external deflector.

The shape of the curves for the nozzle-wing configurations, tend to approach those for a circular nozzle with increasing surface length rather than those for a slot nozzle. This appears to be related to the more circular contour maps associated with the jet flow at the trailing edge for the large wings compared to those for the smaller wings.

CONCLUDING REMARKS

From the data presented, it is apparent that nozzle geometries that provide good jet flow attachment to the wing/flap surface do not necessarily provide good aerodynamic turning efficiencies without adjustments to the nozzle exhaust flow vena contracta. These adjustments can be accomplished by increasing the nozzle size; i.e. exhaust flow area. Such a procedure, however, increases the wetted nozzle surface area resulting in increased nacelle drag for cruise. The least flow problems were encountered with nozzles equipped with external deflectors. In the present study this type nozzle was not optimized. Consequently, the lift-to-thrust values were generally not as beneficial as those for the nozzles without external deflectors.

Considering the acoustic characteristics of the various configurations tested[1], the nozzles with large nozzle roof and sidewall cutback angles had lower noise levels than those with small nozzle roof and sidewall cutback angles. Use of nozzles with large roof angles, however, would imply prohibitively large values of boattail drag for cruise.

The preceding considerations suggest that an optimum OTW nozzle configuration, from all points of view, should consist of a variable nozzle geometry. Such a nozzle design could yield optimized performance for cruise while at the same time providing the necessary low speed aerodynamics and acoustics.

APPENDIX A. - DATA NORMALIZATION

The present study showed that the weight flows of the nozzles-only and nozzle/wing configurations were affected by the individual configuration geometry. In order to provide meaningful comparisons of the aerodynamic data, all configurations are compared on the basis of a common weight flow. In the present study, this was accomplished in the analysis by scaling up the nozzle area of the configurations until the weight flow was equal to that for ideal flow. The following section discusses the validity of this procedure.

The validation of using weight-flow corrected parameters was examined with the 40/40 nozzle and the 3/2-baseline wing. The weight-flow reduction for this nozzle/wing configuration was one of the most severe of all the configurations (fig. 7). Two 40/40 nozzles were constructed similar to that used in the main part of the program (fig. 5(e)). They had exhaust areas 0.16 and 0.30 greater than that of the original nozzle. The nozzle/wing configurations were tested at a nominal M_j of 0.8. The weight flow for each configuration should scale substantially with the nozzle exhaust area. The following relative W/A values were measured with the nozzles at 0.21 chord: original nozzle/wing, 1.267; 16% larger nozzle/wing, 1.252; and 30% larger nozzle/wing, 1.288. From these measurements it is obvious that the weight flow increased at substantially the same rate as the increase in nozzle exhaust area. The lift and thrust values components were measured for these nozzle/wing configurations. The following are the measured L_T/W and T/W values corresponding to the three nozzle/wing configurations used.

Nozzle/Wing Configuration	L_T/W	T/W
1.0 area nozzle	12.7	17.4
1.16 area nozzle	11.3	17.2
1.3 area nozzle	11.1	17.4

The essentially constant values of L_T/W and T/W indicate that the lift and thrust can be scaled on the basis of weight flow.

APPENDIX B. - TRAILING-EDGE VELOCITY CONTOURS

In reference 1, velocity contour maps at the flap trailing edge are given for many of the nozzle-wing configurations included herein. In the following section, a brief review of the major aerodynamic trends evident from these contours will be summarized in order to help complete the documentation of the aerodynamic characteristics of the various nozzle-wing configurations tested. Also included is a brief description of the flow patterns over the wing surfaces.

Velocity contours. - Representative velocity contour maps illustrating the flow field changes at the wing trailing-edge location caused by alterations in geometry are shown in figures 17 to 21. The velocity data, taken from reference 1, are shown in terms of constant local Mach number lines in a spanwise plane normal to the wing surface at the wing trailing edge. Velocity profiles (in terms of local Mach number) in this plane were determined

at the nozzle centerline in a direction perpendicular to the wing surface. The data trends are summarized as follows:

(1) The effect of increasing the nozzle roof angle was to decrease the thickness of the jet shear layer at the nozzle roof angle was to decrease the thickness of the jet shear layer at the wing trailing edge and, at the same time, decrease the peak local Mach number (fig. 17). These changes were accompanied by greater spanwise spreading of the jet flow for constant local Mach number contour lines.

(2) For constant nozzle roof angles, an increase in nozzle sidewall cutback reduced the thickness of the jet shear layer and decrease the peak local Mach number (fig. 18). At the same time, cutback of the nozzle sidewalls also somewhat increased the spanwise spreading of the jet flow at the flap trailing edge.

(3) The effect of wing size on the aerodynamic characteristics is shown in figures 19 and 20. With increasing wing size, the spanwise spread of the jet flow is decreased while the jet shear layer thickness is increased. At the same time, the peak local Mach number at the wing trailing edge decreases with increasing wing size. The effect of locating the nozzles closer to the trailing edges of the wings (0.46 chord, not shown) was to decrease the thickness of the jet shear layer and increase the peak local Mach number in the same manner as decreasing the overall wing size with the nozzles fixed at 0.21 chord. The flow contours at the 0.46 chord location for nozzles with roof angles of 10° and 20° indicated some tendency for the flow to separate off the wing surface at the trailing edge[1].

(4) A comparison of the flow fields obtained at the wing trailing edge with the 40/40 nozzle and those obtained with the simple 5:1 slot nozzle using the 40° full-lip deflector is shown in figure 21. It is apparent that the flow fields with the external deflector configuration have a much thinner jet shear layer and lower peak local Mach numbers than those with the cutback nozzle. The spanwise spread of the jet flow is exceedingly large with the external deflectors compared with that using non-external deflector nozzles.

A reduction in the deflector lip size (full-lip to 1/2-lip) or a reduction in the deflector angle caused both the jet shear layer thickness and peak local Mach number to increase.

Flow visualization. - Limited flow visualization studies were made in order to evaluate in a qualitative manner the degree of flow attachment for some of the nozzle/wing configurations. The method used was to inject a small stream of water (0.16 cm diameter tube) into the jet flow at the nozzle exhaust plane. The point of injection was made at various locations along the perimeter of the nozzle. In figure 22 representative overall flow patterns, obtained by visually observing the water streamers on the wing/flap surface with an M_j of 0.8, are sketched to indicate the primary patterns observed. With a 20° flap deflection, most nozzle configurations provided a wide-spread, well-attached flow pattern as indicated by the dash lines in the figure. With a 60° flap detection, the surface flow pattern just downstream of the nozzle exhaust plane tended to spread out more than with the 20° flap deflection, as shown by the solid curves in figure 22. With nozzle configurations for which the jet flow appeared to be partially detached from the surface the flow pattern curved inward toward the centerline very rapidly, as shown by the dash-dot lines in figure 22, and left the flap trailing edge concentrated in a narrow region. The latter pattern is that associated with the type of velocity contour shown in figure 21(d).

NOMENCLATURE

D_e	equivalent nozzle diameter
h	nozzle height
h*	normalized nozzle height (defined in text)
L	wing/flap surface length
ℓ	wing chord length upstream of nozzle exhaust plane
L_s	projected surface shielding in length
L_T	lift
M	local Mach number
M_j	jet exhaust Mach number
M_p	peak Mach number at flap trailing edge
T	thrust
U_m	peak flow velocity at flap trailing edge
U_j	jet exhaust velocity
W	weight flow
δ	measured local shear layer height at trailing edge
δ_e	measured shear layer height at 0.5 U_m at trailing edge
δ^*	normalized shear height at flap trailing edge
X	axial distance downstream of nozzle exhaust plane
Y,y	wing coordinate system dimensions, see fig. 4
Z	geometry correlation parameters (defined in text)
α	flap deflection angle
β	nozzle roof angle
γ	nozzle sidewall cutback angle
θ	deflector lip angle

Subscripts

i	ideal
V	vectored

REFERENCES

1. von Glahn, U., and Groesbeck, D., "Geometry Effects on STOL Engine-Over-the-Wing Acoustics With 5:1 Slot Nozzles," TM X-71820, 1975, NASA.

2. Reshotko, M., and Friedman, R., "Acoustic Investigation of the Engine-Over-the-Wing Concept Using a D-Shaped Nozzle," TM X-71419, 1973, NASA.

3. Reshotko, M., Olsen, W. A., and Dorsch, R. G., "Preliminary Noise Tests of the Engine-Over-the-Wing Concept. I. 30°-60° Flap Position," TM X-68032, 1972, NASA.

4. Reshotko, M., Olsen, W. A., and Dorsch, R. G., "Preliminary Noise Tests of the Engine-Over-the Wing Concept. II 10°-20° Flap Position," TM X-68104, 1972, NASA.

5. von Glahn, U., and Groesbeck, D., "OTW Noise Correlation for Variations in Nozzle/Wing Geometry With 5:1 Slot Nozzles," AIAA paper 76-521, 1976, Palo Alto, Calif.

6. Groesbeck, D. E., von Glahn, U. H., and Huff, R. G., "Peak Axial-Velocity Decay with Multi-Element Rectangular and Triangular Nozzles," TM X-68047, 1972, NASA.

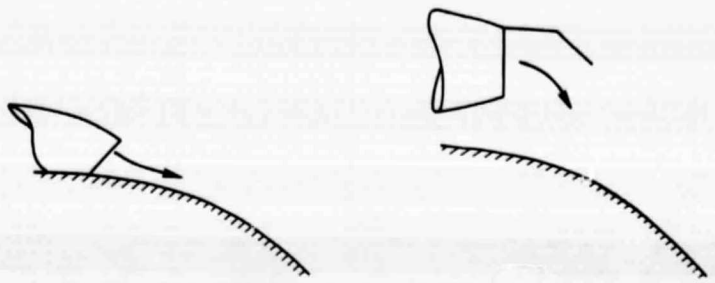

(a) NOZZLE ON-THE-WING; INTERNAL FLOW DEFLECTOR.

(b) NOZZLE ABOVE-THE-WING EXTERNAL FLOW DEFLECTOR.

Figure 1. - Schematic sketches of representative OTW nozzle/wing configurations.

E-8758

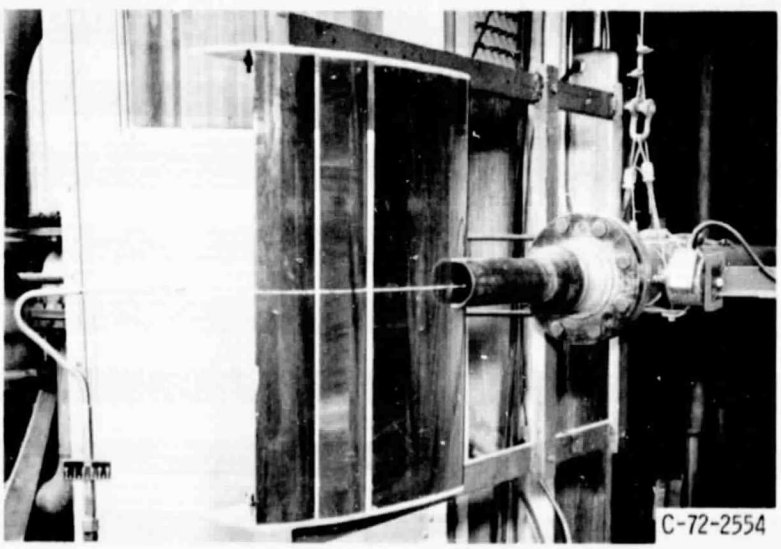

Figure 2. - D-shaped nozzle over the wing without deflector in the lift-thrust facility. 10^0-20^0 flap setting.

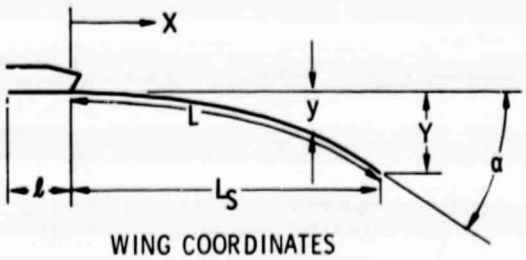

WING COORDINATES

FLAP ANGLE, α, DEG	WING CONFIGURATION	x/L_S / y/Y	0-0.4	0.5	0.6	0.7	0.8	0.9	0.95	0.975	1.0
20	2/3-BASELINE, BASELINE		C	0.04	0.13	0.26	0.44	0.70	0.85	-----	1.0
	3/2-BASELINE		0	.025	0.10	0.225	0.42	0.7	0.85	-----	1.0
60	ALL		0	0.02	0.055	0.125	0.24	0.44	0.61	0.76	1.0

WING DIMENSIONS

FLAP ANGLE, α, DEG	CONFIGURATION	Y, CM	ℓ, CM	L_S, CM	L, CM
20	2/3-BASELINE	4.4 4.4	4.6 10.2	22.5 16.9	23.3 17.8
	BASELINE	6.6 6.6	6.9 15.2	33.8 25.4	35.4 27.0
	3/2-BASELINE	10.2 10.2	10.2 22.9	50.8 38.1	53.2 40.6
60	2/3-BASELINE	9.6	4.6 10.2	20.3 14.7	25.7 20.3
	BASELINE	14.3 14.3	6.9 15.2	30.5 22.1	38.7 30.2
	3/2-BASELINE	21.5 21.5	10.2 22.9	45.7 33.1	57.6 45.1

Figure 4. - Wing dimensions and coordinates. Dimensions in centimeters.

E-8758

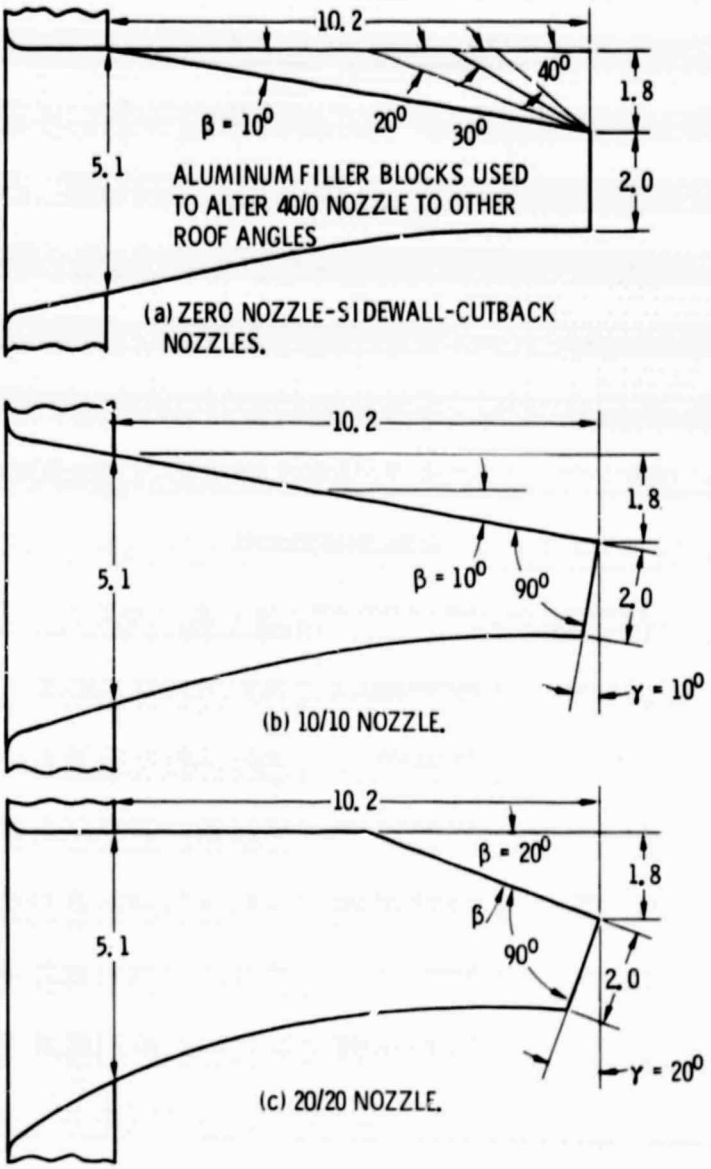

Figure 5. - Sketches of test nozzles and external deflectors. All nozzles were 10.2 cm wide. Dimensions in centimeters.

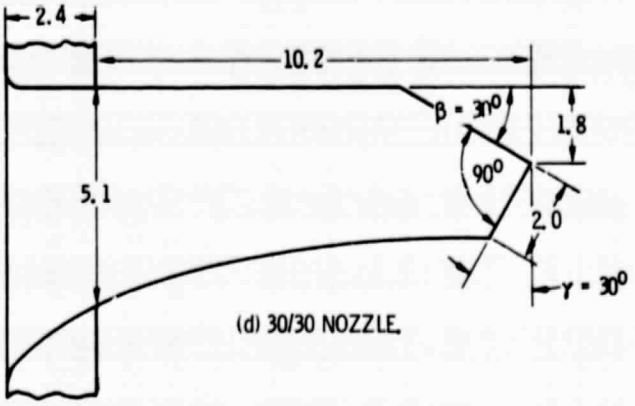

(d) 30/30 NOZZLE.

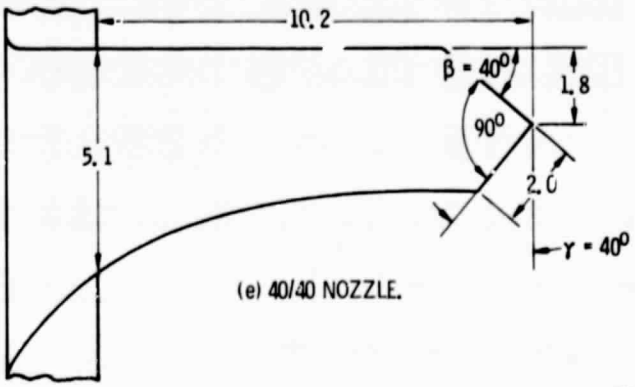

(e) 40/40 NOZZLE.

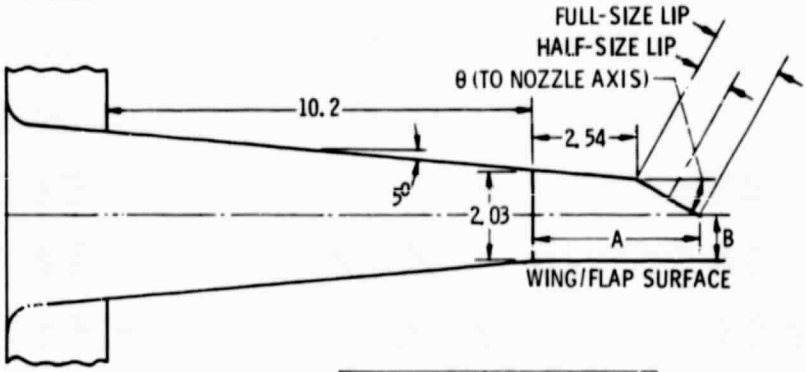

FLAP ANGLE, DEG	WING CONFIG-URATION	ℓ, CM	DEFLECTOR ANGLE, θ					
			30°		40°- FULL LIP		40°- ½ LIP	
			A	B	A	B	A	B
20	BASELINE	6.9	4.0	1.40	3.63	1.30	3.20	1.75
		15.2		1.50		1.40		1.78
60	BASELINE	6.9		1.47		1.40		1.83
		15.2		1.52		1.42		1.93

(f) DEFLECTOR DIMENSIONS WITH BASELINE 5:1 SLOT NOZZLE. ALL DEFLECTORS WERE 15.2 CM WIDE.

Figure 5. - Concluded.

E-8758

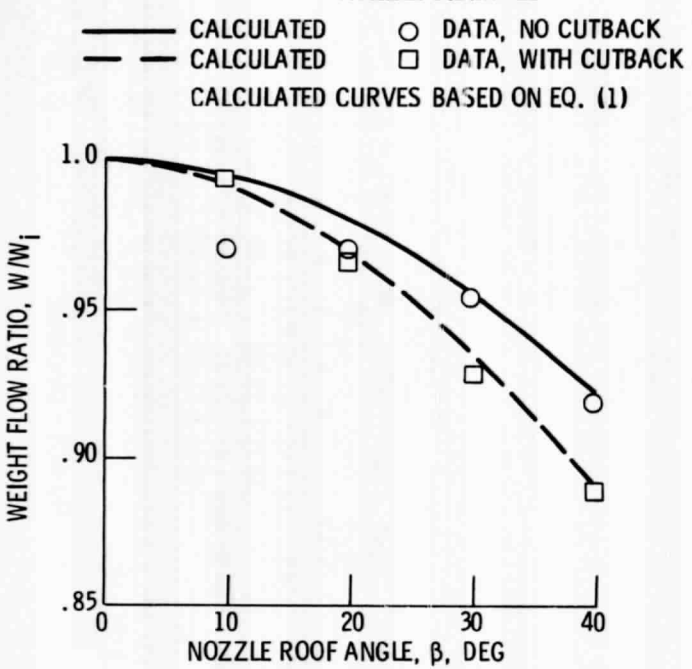

Figure 6. - Weight flow reduction for nozzle-only as function of nozzle roof angle. Calculated ideal weight flow, 0.716 kg/sec; M_j, 0.8.

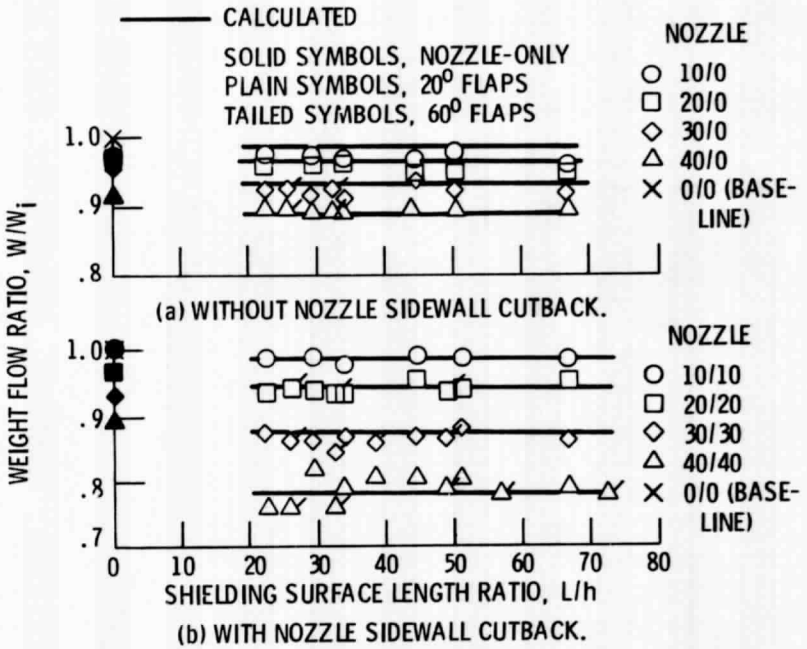

Figure 7. - Comparison of weight flow ratios with calculated values for various nozzle/wing configurations; M_j, 0.8.

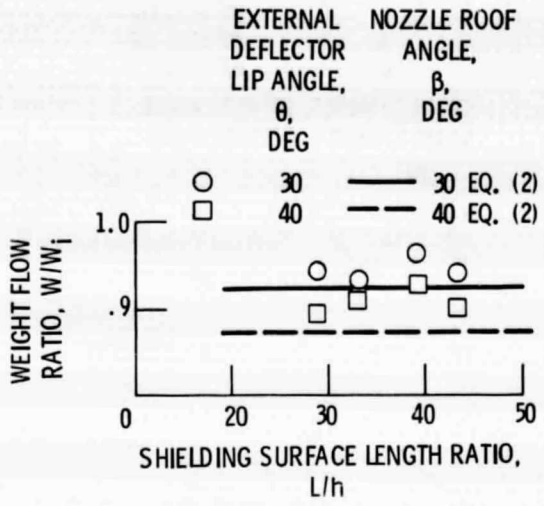

Figure 8. - Comparison of weight flow ratio for nozzle/wing configuration with external deflector and that calculated for nozzle-wing configuration without sidewall cutback. Full-size lip deflector; M_j, 0.8.

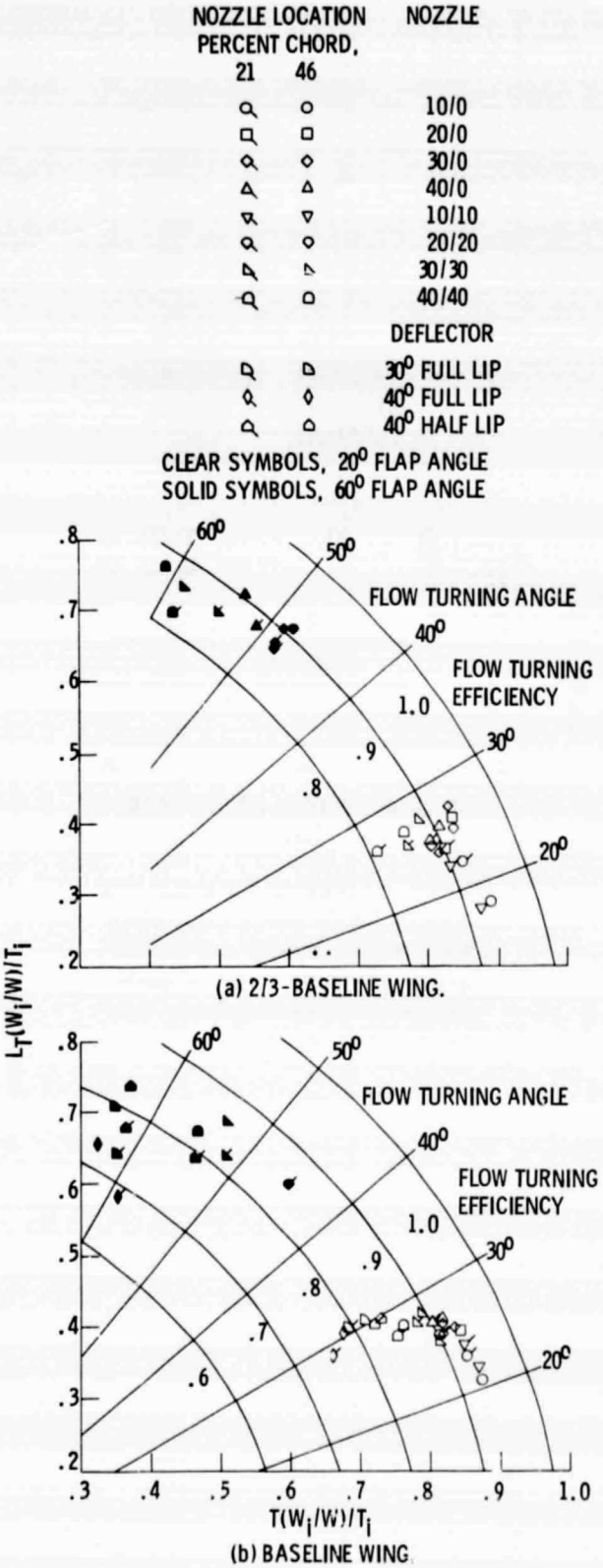

Figure 9. - Static turning effectiveness for various nozzle-wing configurations; jet exhaust velocity, 266 m/sec; $M_j = 0.805$.

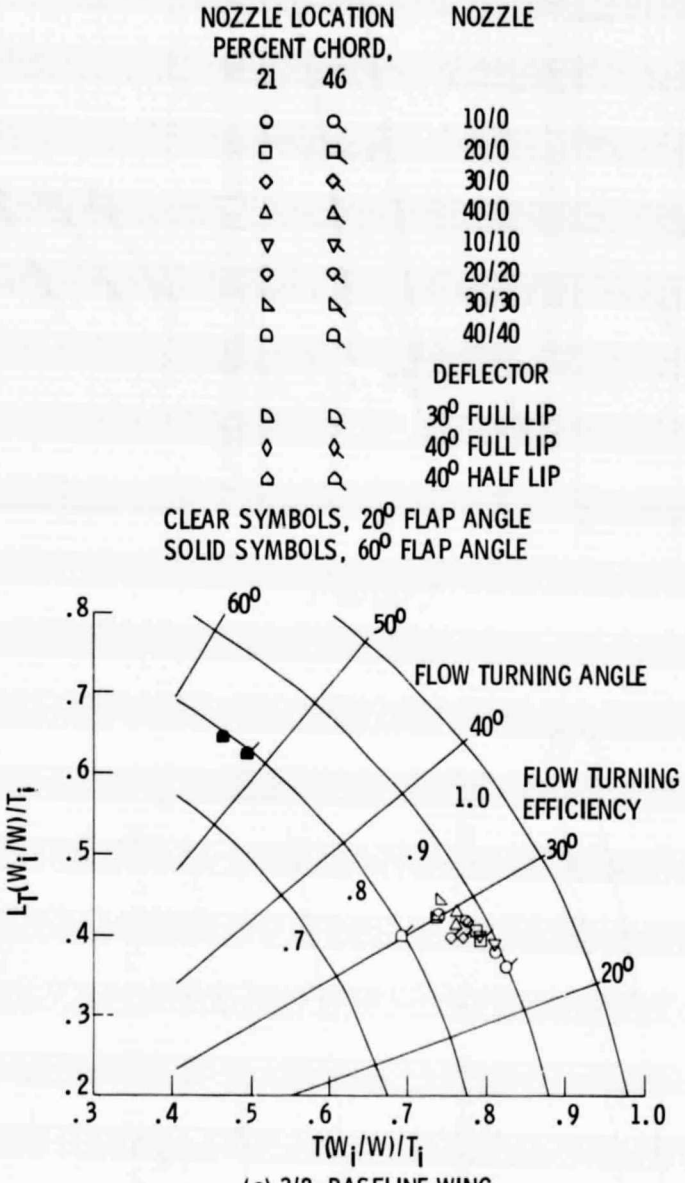

(c) 3/2-BASELINE WING.

Figure 9. - Concluded.

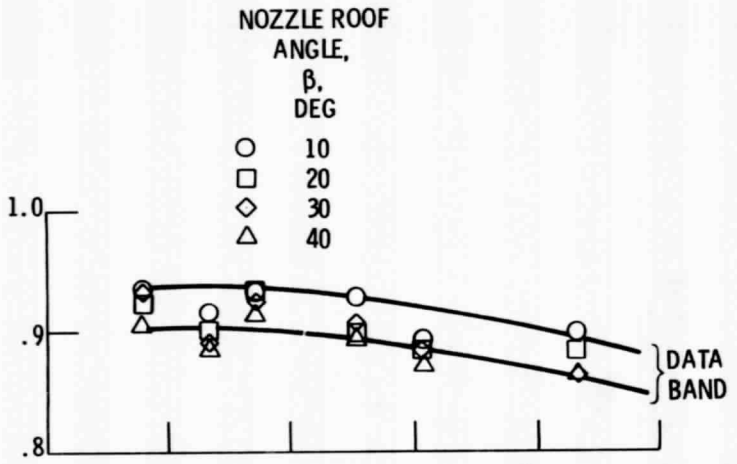

(a) NOZZLE WITHOUT SIDEWALL CUTBACK, 20° FLAP ANGLE.

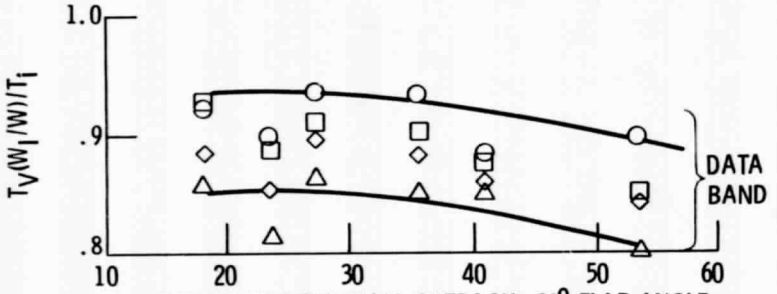

(b) NOZZLE WITH SIDEWALL CUTBACK, 20° FLAP ANGLE.

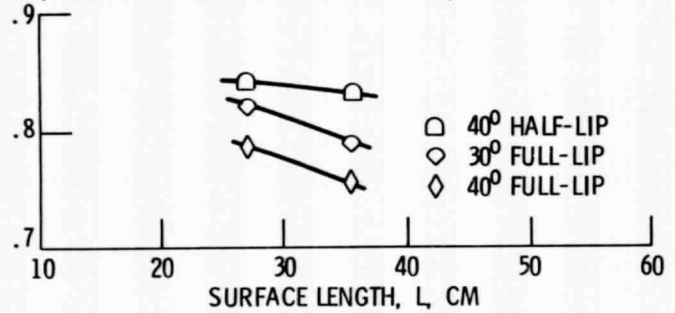

(c) NOZZLE WITH EXTERNAL DEFLECTOR, 20° FLAP ANGLE.

Figure 10. - Variation of vectored thrust with wing size; M_j, 0.8.

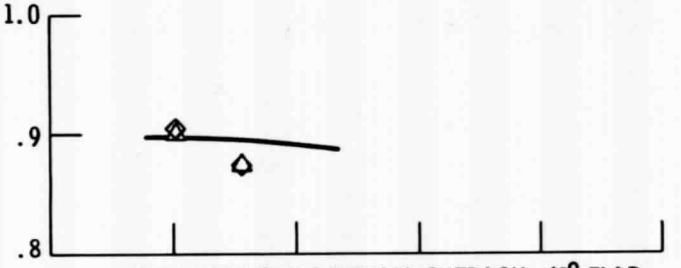

(d) NOZZLE WITHOUT SIDEWALL CUTBACK, 60° FLAP ANGLE.

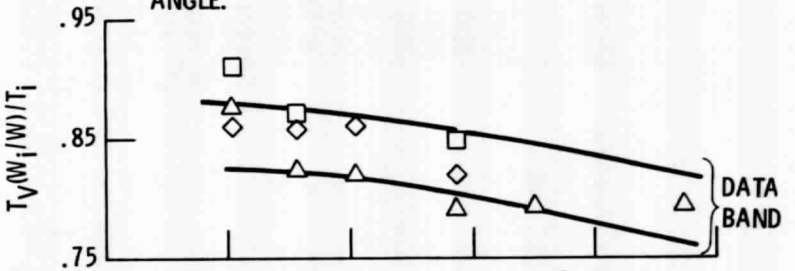

(e) NOZZLE WITH SIDEWALL CUTBACK, 60° FLAP ANGLE.

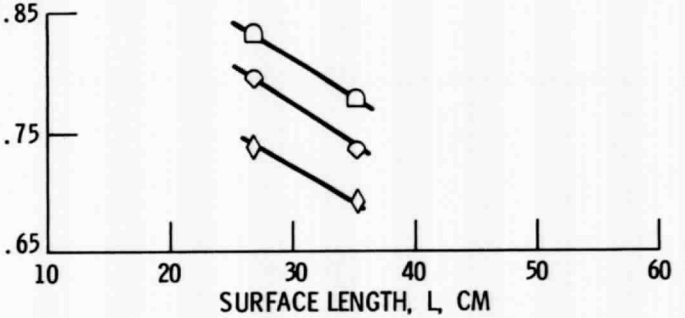

(f) NOZZLE WITH EXTERNAL DEFLECTOR, 60° FLAP ANGLE.

Figure 10. - Concluded.

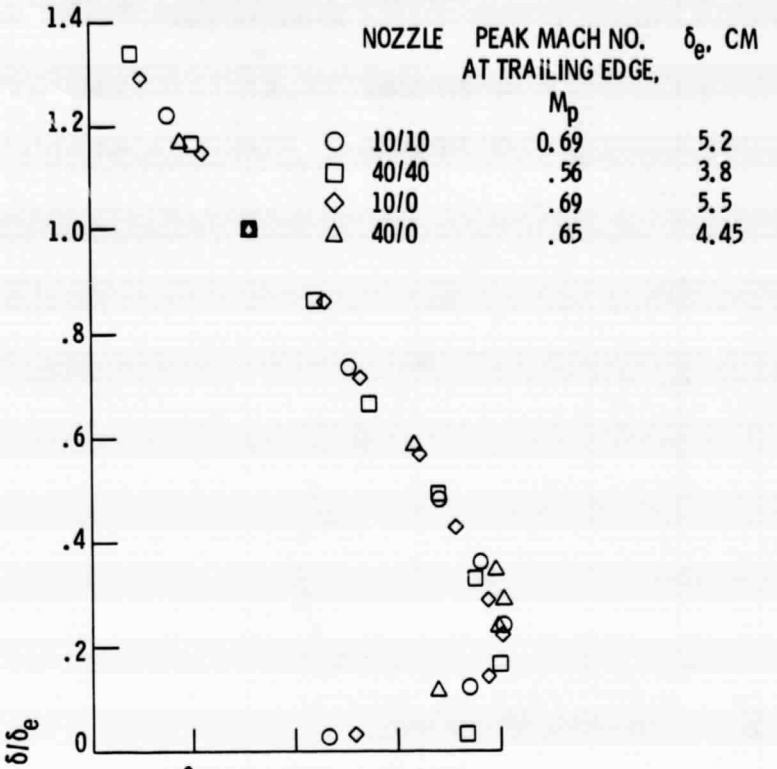

(a) 20^0 FLAP ANGLE; L, 35.4 CM.

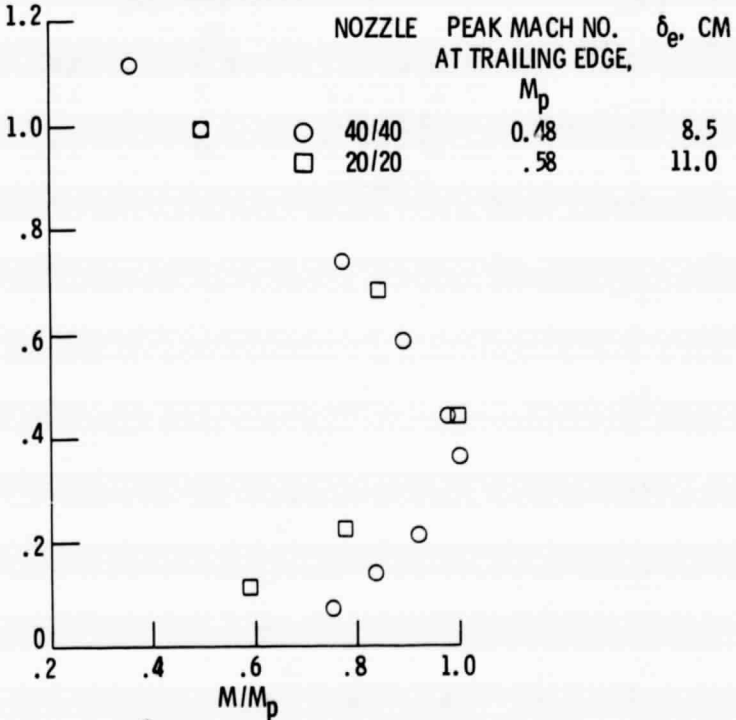

(b) 60^0 FLAP ANGLE; L, 38.7 CM.

Figure 11. - Normalized trailing edge velocity profiles at nozzle centerline; M_j, 0.8; representative data.

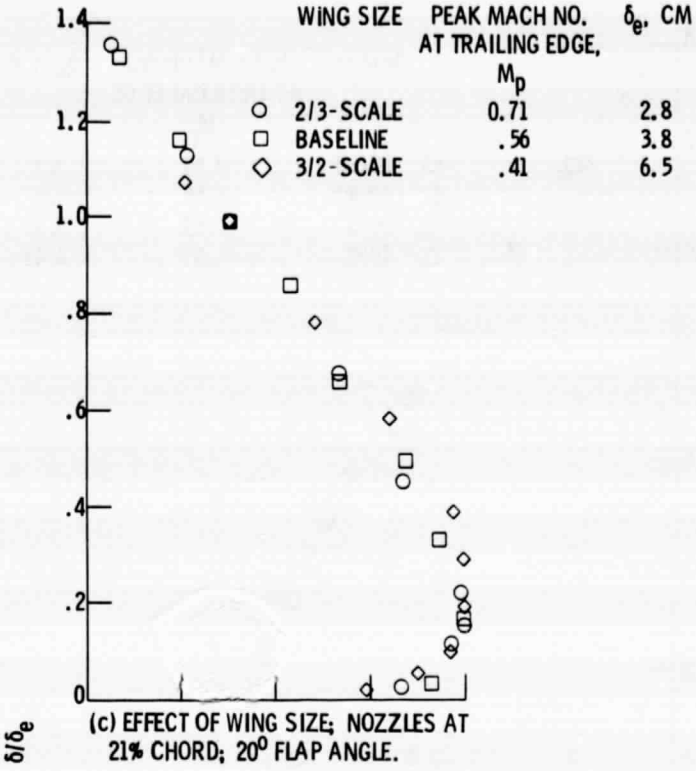

(c) EFFECT OF WING SIZE; NOZZLES AT 21% CHORD; 20° FLAP ANGLE.

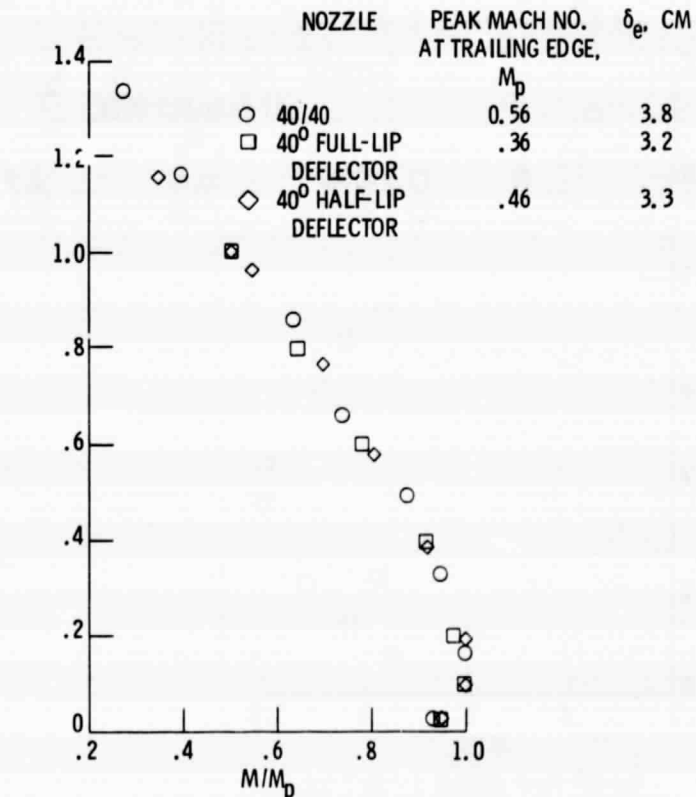

(d) 20° FLAP ANGLE; L, 35.4 CM; EXTERNAL DEFLECTORS.

Figure 11. - Continued.

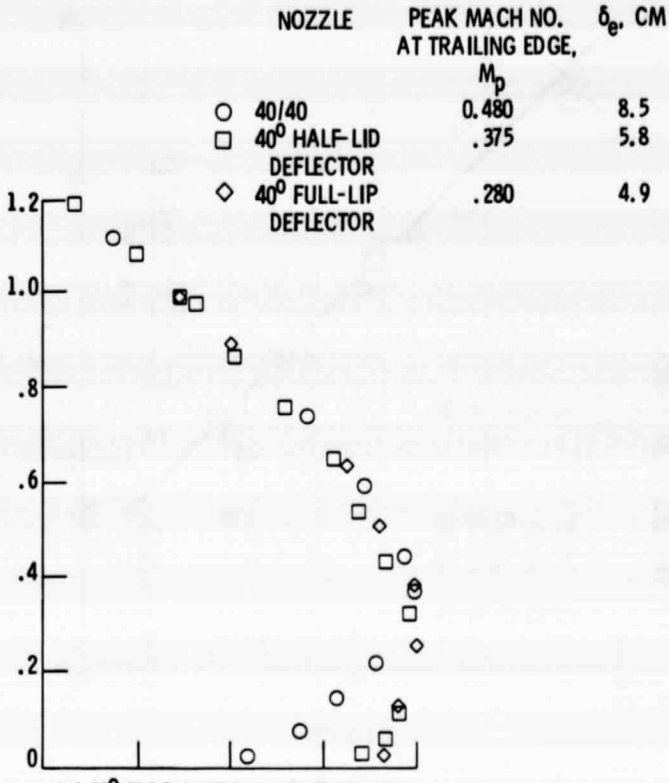

(e) 60° FLAP ANGLE; L, 38.7 CM; EXTERNAL DEFLECTORS.

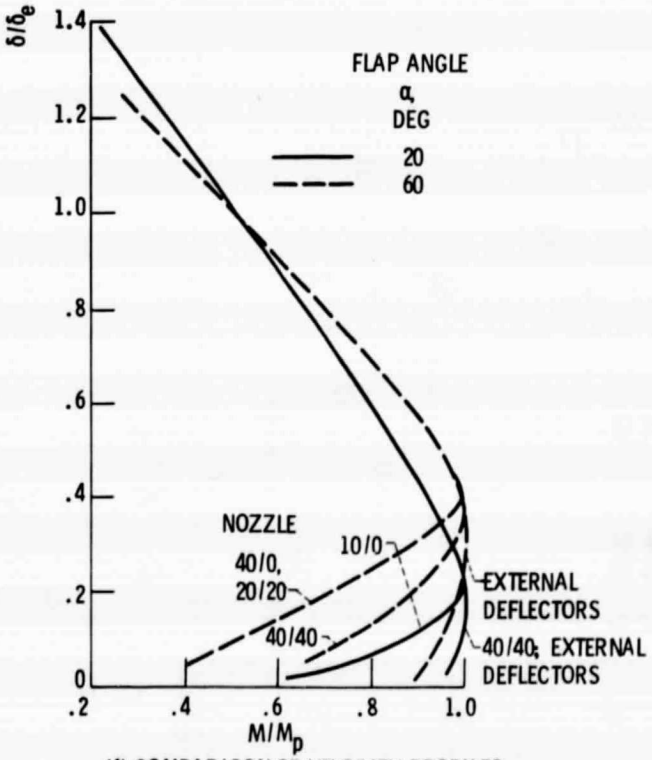

(f) COMPARISON OF VELOCITY PROFILES AT 20° AND 60° FLAP ANGLES.

Figure 11. - Concluded.

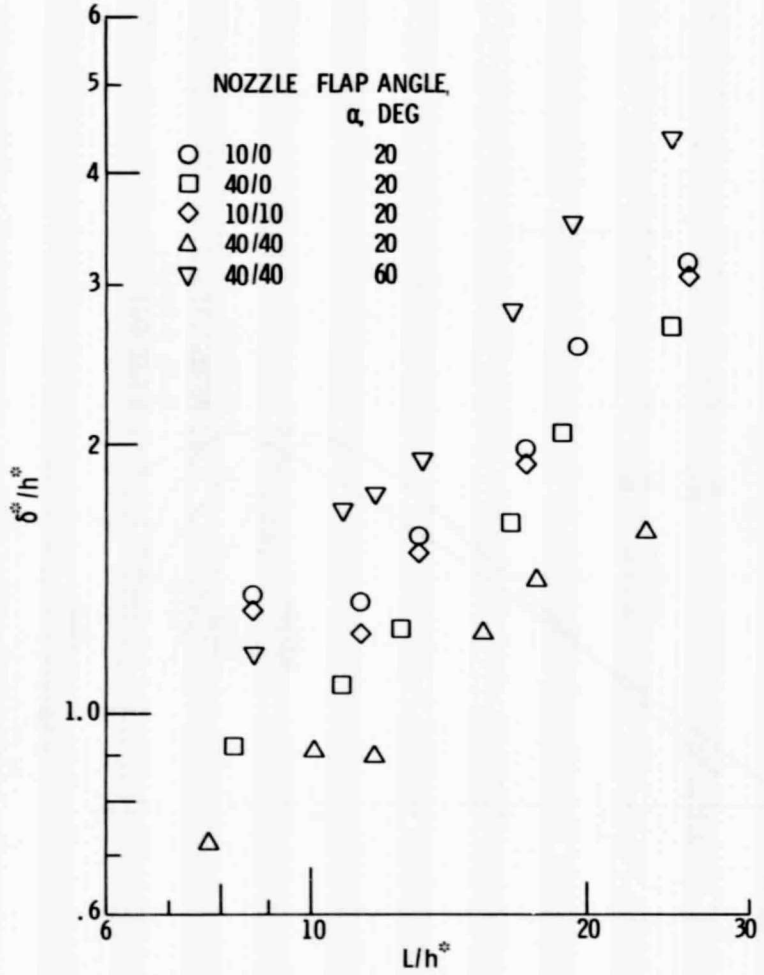

Figure 12. - Representative variations of normalized shear layer height, δ^*, with surface length; M_j, 0.8.

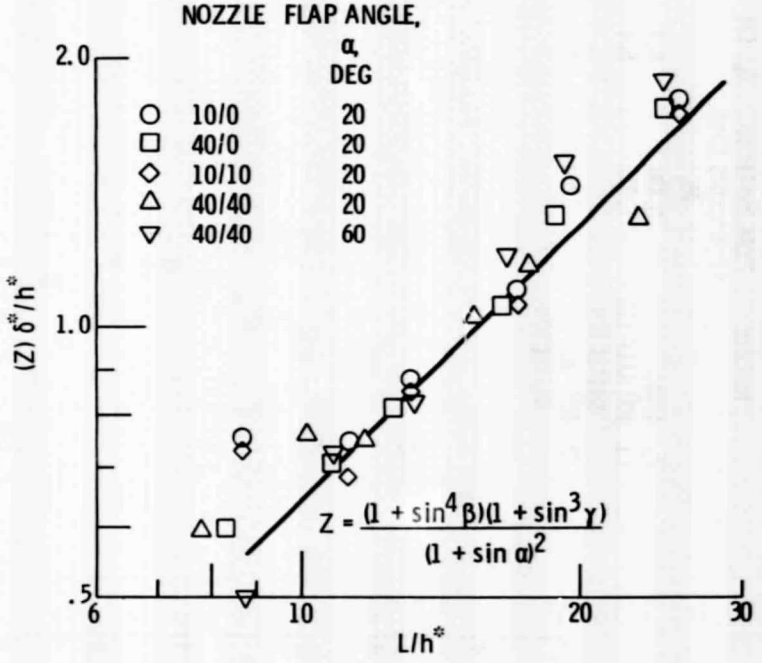

Figure 13. - Correlation of δ^* for nozzle geometry; M_j, 0.8.

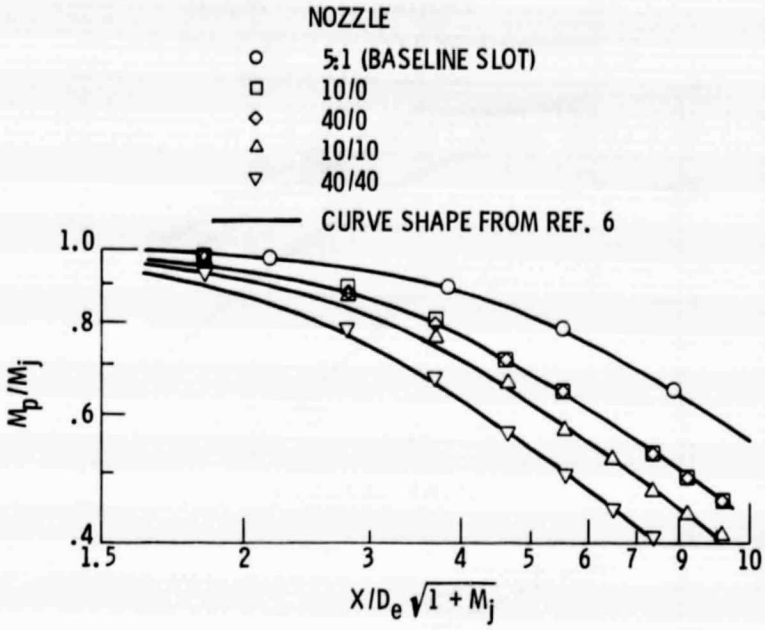

Figure 14. - Representative peak-axial jet velocity decay for several nozzle-only configurations. Nominal jet Mach number, M_j, 0.8.

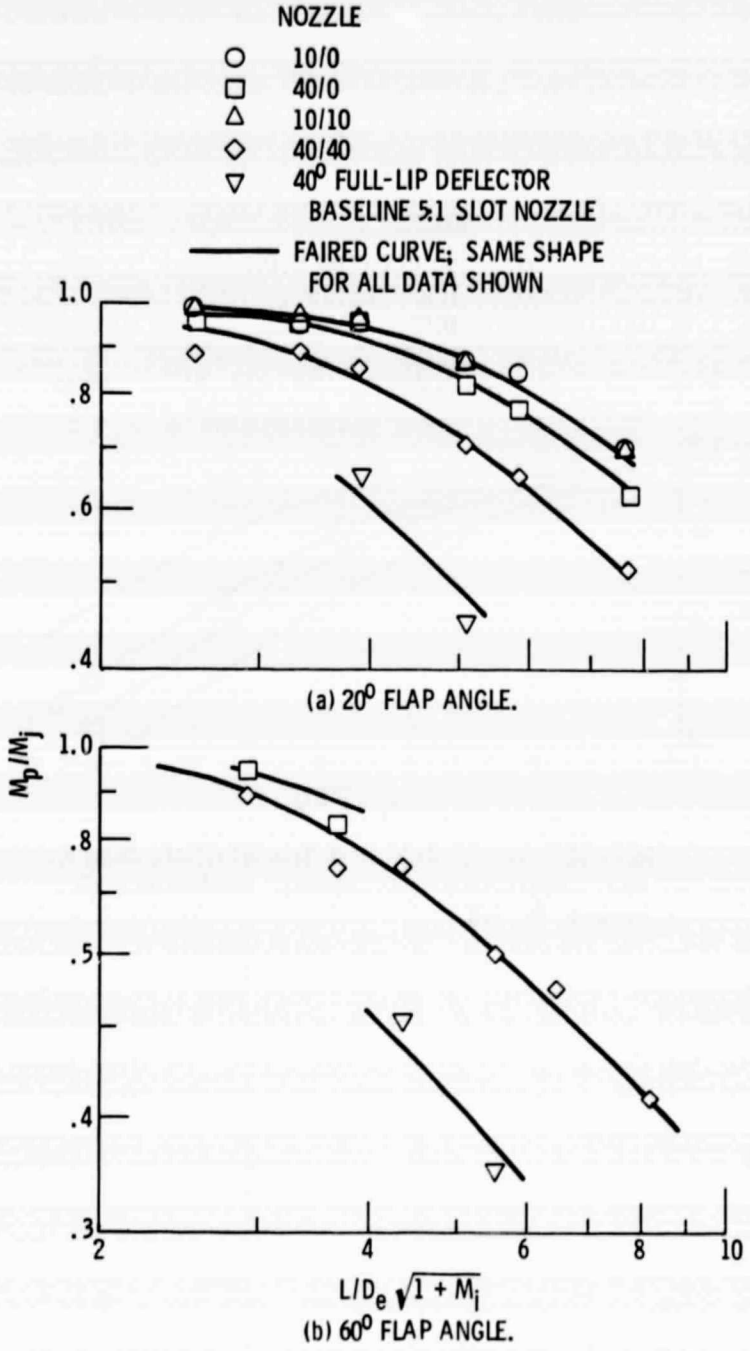

Figure 15. - Peak jet velocity decay at flap trailing edge for representative nozzle/wing configurations. Nominal jet Mach number, M_j, 0.8.

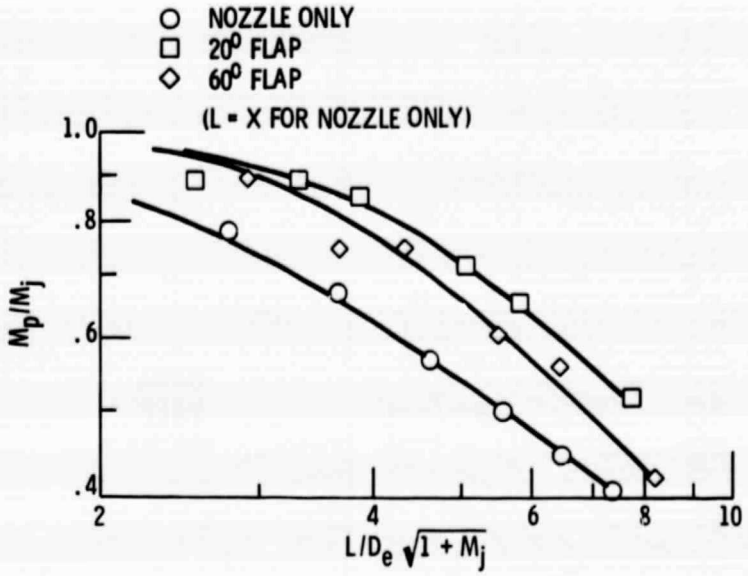

Figure 16. - Comparison of velocity decay for representative nozzle/wing configuration with that for nozzle only, 40/40 nozzle; M_j, 0.8.

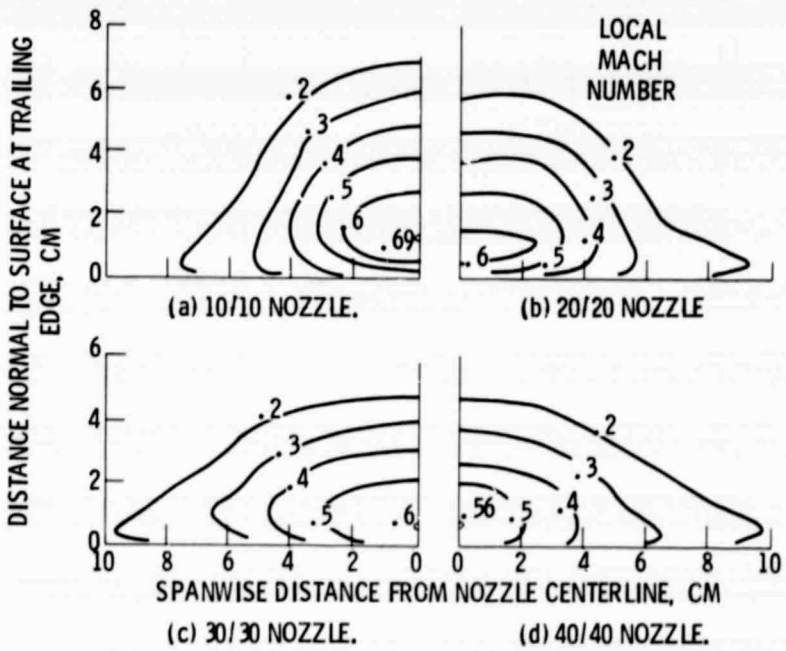

Figure 17. - Flow contour maps at trailing edge for baseline wing with cutback nozzles. 20° flap deflection; U_j, 266 m/sec; nozzles at 0.21 chord.

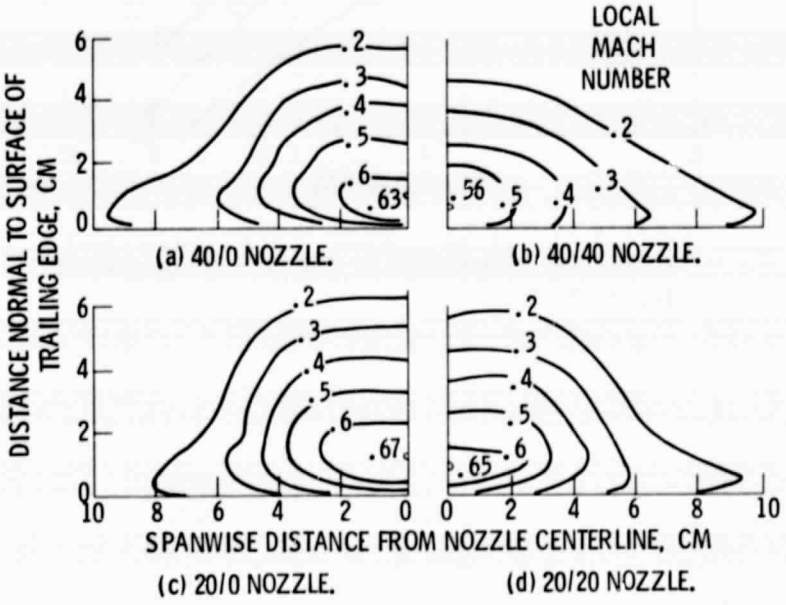

Figure 18. - Comparison of flow contours for baseline wing and nozzles with and without sidewall cutback. 20^{0} flap deflection; U_j, 266 m/sec; nozzles at 0.21 chord.

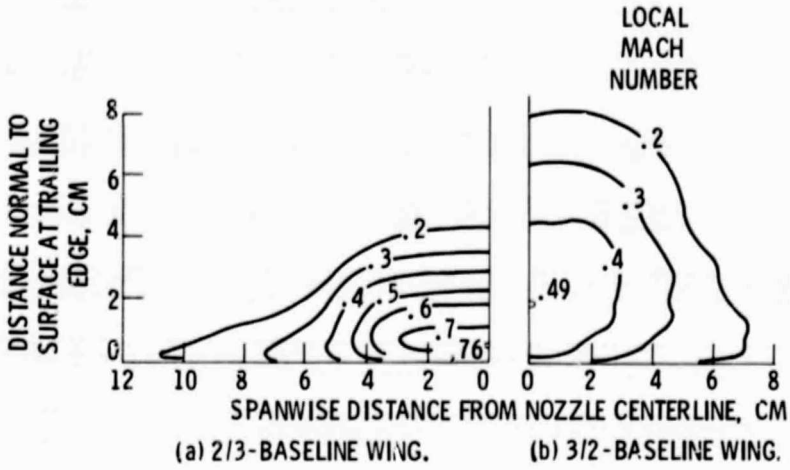

Figure 19. - Comparison of flow contours for two wing sizes using 20/20 nozzle. 20^{0} flap deflection; U_j, 266 m/sec; nozzle at 0.21 chord.

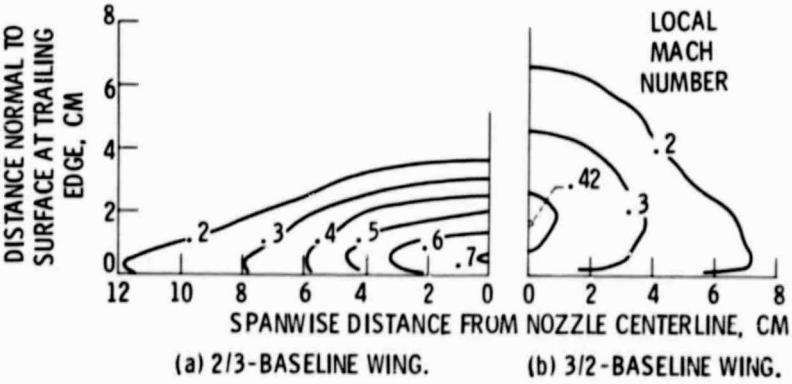

Figure 20. - Comparison of flow contours for two wing sizes using 40/40 nozzle. 20^{0} flap deflection; U_j, 266 m/sec; nozzle at 0.21 chord.

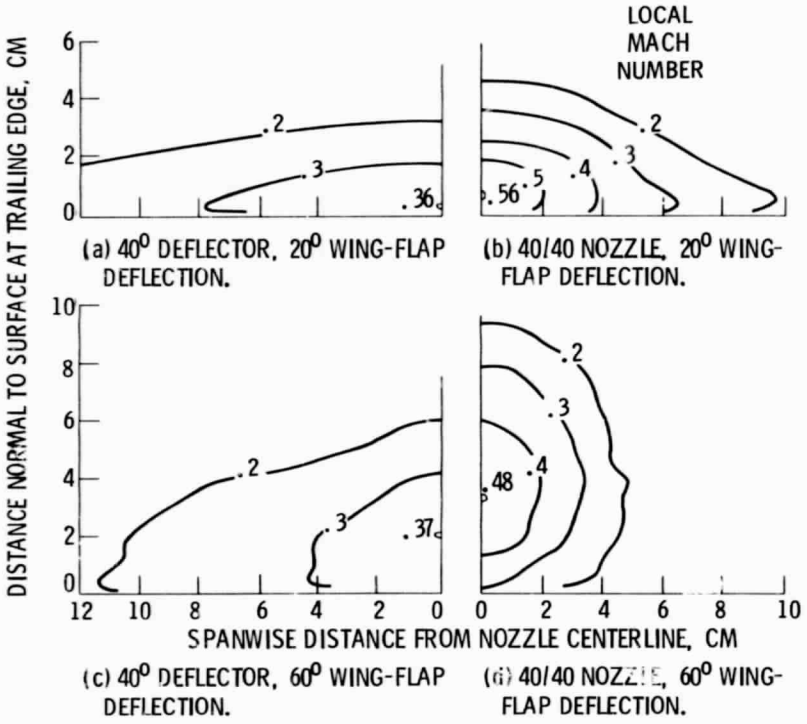

Figure 21. - Comparison of flow contours for baseline wings with 40/40 nozzle and with reference 5:1 slot nozzle using 40° full-lip deflector, U_j, 266 m/sec; nozzles at 0.21 chord.

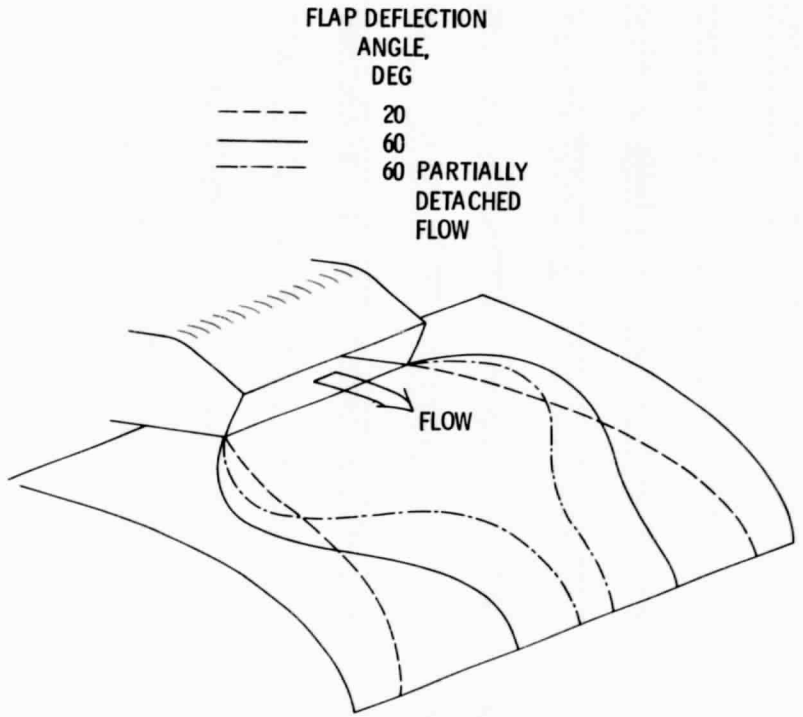

Figure 22. - Schematic sketch of representative jet flow patterns over wing/flap surface; M_j, 0.8.